Available online at www.sciencedirect.com
SciVerse ScienceDirect
Ceramics International 39 (2013) S691–S694
CERAMICS INTERNATIONAL
www.elsevier.com/locate/ceramint

Longitudinal and bending hybrid linear ultrasonic motor using bending PZT elements

Xiaohui Yang*, Yingxiang Liu, Weishan Chen, Junkao Liu

State Key Laboratory of Robotics and System, Harbin Institute of Technology, 2 Yikuang Street, 150001 Harbin, China

Available online 17 October 2012

Abstract

In this study, a new linear ultrasonic motor using bolt-clamped Langevin type transducer with two feet is proposed. In this new design, only the bending vibration ceramics are employed; the longitudinal and bending vibrations of the transducer are excited by adopting a new exciting mode. Two groups of ceramics on both sides of the neutral plane of the bending mode shape are excited by two alternating voltages with phase difference. Then, the vibrations are composed and generate elliptical trajectories at the driving feet. The resonance frequencies of the two vibration modes of the motor are tuned to realize the modal degeneration using finite element method. The prototype motor achieved a maximum speed of 560 mm/s and a maximum output force of 55 N at a voltage of 450 V_{p-p}.

Keywords: C. Mechanical properties; D. PZT; E. Actuators; Linear ultrasonic motor

1. Introduction

Ultrasonic motors (USMs) are a new type actuator via converse piezoelectric effect developed since the 1980s. Ultrasonic motors have received profound attention by their merits of high torque at low speed, compact size, high holding torque with no power consumption, simple structure, high positioning accuracy, no electromagnetic radiation, and so on [1,2]. As a new actuator, ultrasonic motors have been a research hotspot of the current electromechanical control field.

From a vibration characteristic viewpoint, USMs can be classified into a standing-wave type, a travelling-wave type [3] and a composite mode type. Owing to the possibility to realize driving in the two opposite directions, the travelling-wave type and the composite mode type of ultrasonic motors obtain more extensive application. Longitudinal and bending hybrid linear ultrasonic motors discussed in this study belong to the composite mode type. For example, C.H. Yun presented a high power ultrasonic linear motor using a longitudinal and bending hybrid bolt-clamped Langevin type transducer [4] and a piezoelectric ultrasonic linear micromotor using a slotted stator [5] in succession. The latter type motor transforms energy by using the d31 mode. The PZT plates are bonded to a metal substrate to excite longitudinal and bending vibrations. In the former type motor and several ultrasonic motors [6,7] proposed by the authors, PZTs are clamped between metal bars with bolts and work in the d33 mode, which has higher electromechanical coupling efficiency than does the d31 mode.

Compared with the bonded type motors, the bolt-clamped type motors exhibit larger mechanical output force. The new ultrasonic motor in this study also adopts the bolt-clamped type. In the previous ultrasonic motors using longitudinal and bending composite modes, there are usually both longitudinal vibration ceramics and bending vibration ceramics in a longitudinal–bending hybrid transducer. The longitudinal and bending vibrations of the transducer are generated independently. In this study, a new exciting mode is devised. In this new design, the longitudinal and bending vibrations of the transducer are excited by adopting only the bending vibration ceramics. Based on the new design, a new linear ultrasonic motor using bolt-clamped Langevin type transducer is proposed in this study.

2. A new exciting mode

The fundamental principle of the new exciting mode is shown in Fig. 1 and Table 1. A group of bending PZT

*Corresponding author. Tel.: +86 45186417891; fax: +86 45186416119.
E-mail address: youngsme@163.com (X. Yang).

0272-8842/$ - see front matter © 2012 Elsevier Ltd and Techna Group S.r.l. All rights reserved.
http://dx.doi.org/10.1016/j.ceramint.2012.10.163

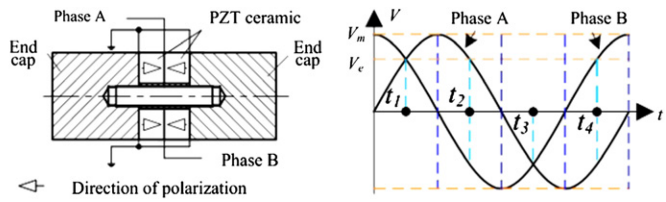

Fig. 1. A bolt-clamped beam with bending PZTs excited by two alternating voltages with 90° phase difference.

Table 1
Vibration shapes of the bolt-clamped beam with the new exciting mode in one cycle

Longitudinal vibration	Bending vibration
$t=t_1$ 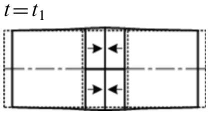	$t=t_2$ 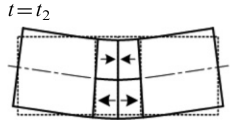
$t=t_3$ 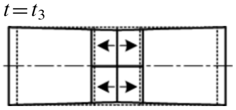	$t=t_4$ 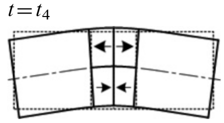

← Direction of deformation

ceramics are fastened between two end caps by a bolt. Each bending PZT is cut into two parts. The polarization directions of bending PZTs are along the axial direction of beam. As seen from Fig. 1, two adjacent halves of bending PZTs with the opposite polarization directions are excited by one phase voltage. Phase A and phase B are two alternating voltages, which have 90° phase difference in Fig. 1. When $t=t_1$ or $t=t_3$, $V_A=V_B$, the bolt-clamped beam is in the extreme positions of longitudinal vibration. When $t=t_2$ or $t=t_4$, $V_A=-V_B$, the extreme positions of bending vibration are presented.

In the new exciting mode, longitudinal and bending vibrations are not independent, and the two vibrations are totally hybrid. Most important of all is that employing only bending PZT can generate both longitudinal and bending vibrations. This is different from the classical exciting mode with longitudinal vibration ceramics and bending vibration ceramics, where when the applied voltage is V_e rather than V_m (when $|V_A(t)|=|V_B(t)|$, $V_e=|V_A(t)|$, and V_m is the amplitude of phase A and phase B, as shown in Fig. 1), vibration displacements of the motor in horizontal and vertical directions are maximum.

3. Construction and operating principle

3.1. Motor structure

The three-dimensional model of the proposed motor is shown in Fig. 2. Two exponential shape horns are located on the two ends to magnify vibration amplitude and velocity. Two groups of bending PZT ceramics are sandwiched between flange bolt and horns, whose polarization is also given in Fig. 2. Beryllium bronze sheets are clamped to serve as electrodes. The friction material blocks serving as the driving feet, are bonded on the end tips of the horns, which are located in the same side of the transducer. There are two clamping holes in the middle of the flange to fix the motor and apply preload. The proposed motor forms elliptical trajectories at the driving feet by superimposing longitudinal and bending vibrations with phase difference temporally.

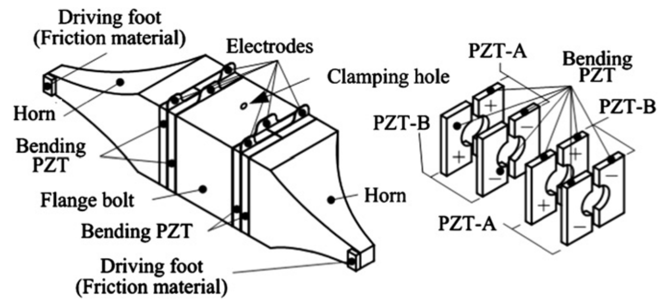

Fig. 2. Structure of the proposed motor using the new exciting mode.

3.2. Motor driving principle

In the proposed motor, bending ceramics PZT-A and PZT-B are excited by two alternating voltages with different phases. Then, the stretching vibration of PZT ceramics is excited via converse piezoelectric effect. Two groups of bending PZT ceramics are located at the wave loops of bending mode wave on the transducer, which ensures effective excitation of the bending vibration of the motor. As shown in Fig. 3, the fourth-order bending vibration mode and the first-order longitudinal vibration mode of the transducer are adopted.

When the displacements of the two tips have 90° phase difference spatially in OX and OY directions, elliptical motion trajectories with the same rotation direction can be generated on the end tips, as Fig. 3 shows. The two driving tips drive the runner by the frictional forces between them. When the phase difference is spatially altered to be $-90°$, the reverse frictional forces result in the reverse motion of the runner.

4. Design and analysis of the motor

4.1. Modal degeneration

For the excitation of elliptical trajectories on the two driving tips, the resonance frequencies of the longitudinal and bending modes of the motor should be close to each other. The finite element model of the motor is founded in ANSYS. Aluminum is the selected material of the horns. Steel is the selected material of the flange bolt. The PZT ceramics material is PZT-4. The electrodes are ignored since they are too thin to be meshed. And the friction blocks serving as the driving feet are also ignored because of their tiny mass. Fig. 4 shows the section view of the motor.

During the modal analysis, SOLID227 element is used for the meshing. Modal degeneration can be obtained by mean of adjusting the structural parameters of the motor. Fig. 4 also lists the final structural parameters of the motor and modal analysis results show that the resonance frequencies of the first-order longitudinal mode and the fourth-order bending mode are 27.825 kHz and 27.742 kHz, respectively. The two resonance frequencies are different. There is a discrepancy of 83 Hz, which states the good degeneration of the longitudinal and bending modes.

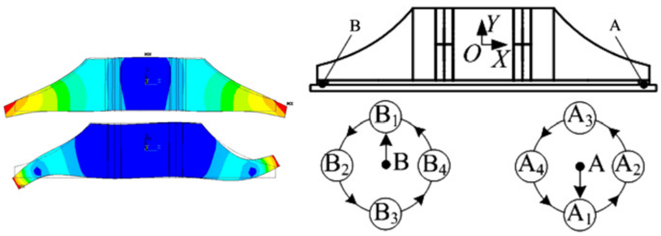

Fig. 3. Vibration modes of the motor and schematic diagram of working principle.

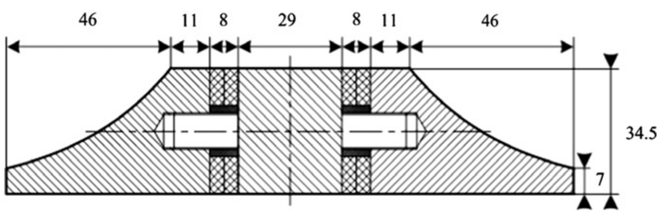

Fig. 4. Section view and the final structural parameters of the motor (unit: mm).

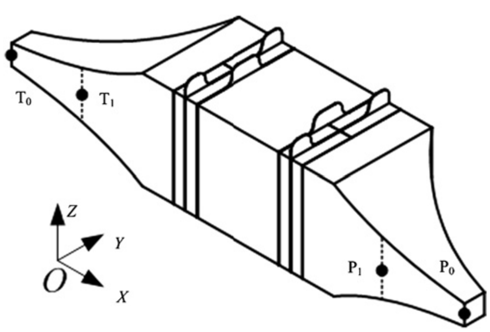

Fig. 5. Schematic diagram of nodes selection.

4.2. Vibration characteristic analysis

The vibration characteristics of the proposed motor are obtained by transient analysis. Two alternating voltages (the frequency is 27.784 kHz, the virtual value is 100 V, and the phase difference is 90°) were applied on the PZT ceramics to accomplish the transient analysis. To gain the vibration characteristics of the driving tips, two nodes of the end tips of the horns (P_0 and T_0) and two nodes on the location of wave loops of bending vibration (P_1 and T_1) were selected, as Fig. 5 shows. Fig. 6(a) gives the motion trajectories of the selected nodes in the last simulation cycle.

Fig. 6(a) indicates that the motion trajectories of the selected nodes are ellipses in the *XOY* plane, which is coincident with the working principle shown in Fig. 3. The maximum displacements of P_0 and T_0 in *OX* and *OY* directions are 5.83 μm and 12.47 μm respectively which are much larger than the one of P_1 and T_1. Obviously, P_0 and T_0 are more appropriate for driving the runner. However, the motion trajectories are oblique ellipses inconsistently which have bad influence on the mechanical performance. By changing the phase difference of two exciting voltages, the motion trajectories can be improved. When the phase difference of the exciting voltages is altered to be 60°, the motion trajectories of P_0 and T_0 in the last simulation cycle are shown in Fig. 6(b). The maximum displacements

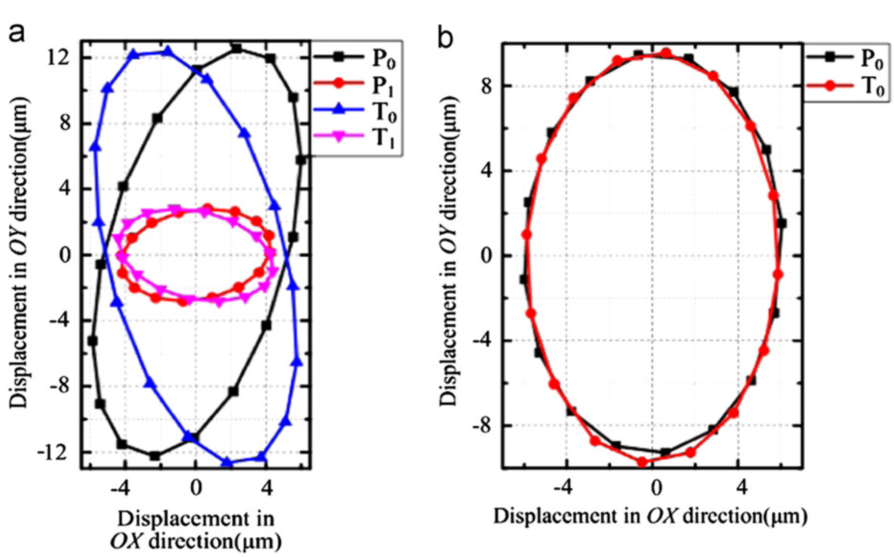

Fig. 6. Motion trajectories of the selected nodes: (a) 90° phase difference and (b) 60° phase difference.

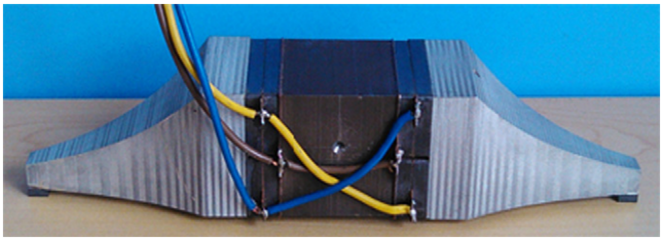

Fig. 7. Prototype motor.

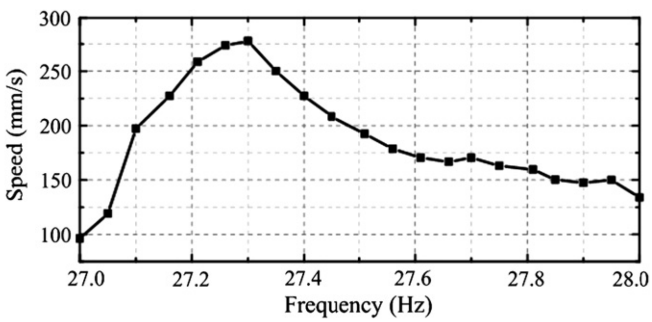

Fig. 8. Plot of the speed of motor versus the exciting frequencies.

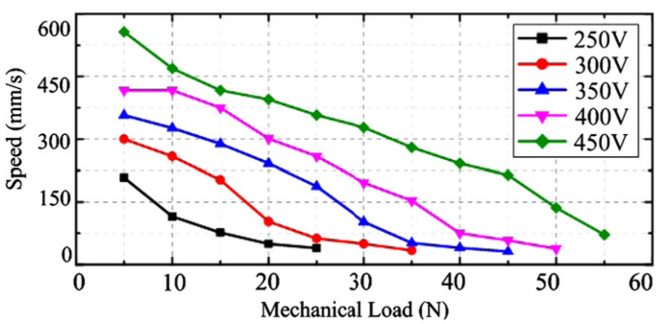

Fig. 9. Load characteristics for various exciting voltages.

of P_0 and T_0 in OX and OY directions are 5.95 μm and 9.53 μm respectively. The driving direction of the motor can reverse when two alternating voltages have -60° phase difference.

5. Experiments

A prototype motor was fabricated according to the geometrical parameters listed in Fig. 4. Fig. 7 shows photo of the prototype motor.

The mechanical output characteristics of the prototype motor are tested using the experiment set-up developed by a previous study [8]. The speed of the motor against the exciting frequency curve is shown in Fig. 8, while the voltages (peak-to-peak) are 250 V, the phase difference of the exciting voltages is 60° and the preload is 250 N. The maximum speed of 278 mm/s is obtained at the frequency of 27.3 kHz. Fig. 9 shows the plot of the speed and mechanical load for various exciting voltages at a preload of 250 N and the frequency of 27.3 kHz, while the phase difference of the exciting voltages is 60°. When the voltage (peak-to-peak) is 450 V, the maximum speed and the maximum mechanical output force of the motor are 560 mm/s and 55 N, respectively.

6. Conclusions

A longitudinal and bending hybrid linear ultrasonic motor using bending PZT elements was proposed in this study. The new exciting mode was analyzed. The vibration modes of the motor were obtained by modal analysis and the motion trajectories of the motor were analyzed by transient analysis. A prototype motor was fabricated and measured. Typical output of the prototype is maximum speed of 560 mm/s and maximum output force of 55 N at two alternating voltages of 450 V_{p-p} with 60° phase difference. The driving direction of the motor can reverse when two alternating voltages have -60° phase difference. The prototype motor verifies the feasibility of the new exciting mode. The new exciting mode can be utilized with many other longitudinal and bending hybrid ultrasonic motors.

Acknowledgment

This project is supported by the National Natural Science Foundation of China (nos. 50875057 and 51105097) and the Research Fund for the Doctoral Program of Higher Education of China (no. 20102302110007).

References

[1] S. Ueha, Y. Tomikawa, M. Kurosawa, N. Nakamura, Ultrasonic Motors Theory and Applications, Clarendon Press, Oxford, UK, 1993.

[2] C.S. Zhao, Ultrasonic Motors Technologies and Application, Science Press, Beijing, China, 2007.

[3] K. Uchino, Piezoelectric ultrasonic motors: overview, Smart Materials and Structures 7 (1998) 273–285.

[4] C.H. Yun, T. Ishii, K. Nakamura, S. Ueha, K. Akashi, A high power ultrasonic linear motor using a longitudinal and bending hybrid bolt-clamped Langevin type transducer, Japanese Journal of Applied Physics 40 (2001) 3773–3776.

[5] C.H. Yun, B. Watson, J. Friend, L. Yeo, A piezoelectric ultrasonic linear micromotor using a slotted stator, IEEE Transactions on Ultrasonics, Ferroelectrics and Frequency Control 57 (2010) 1868–1874.

[6] Y.X. Liu, W.S. Chen, J.K. Liu, S.J. Shi, A cylindrical traveling wave ultrasonic motor using longitudinal and bending composite transducer, Sensors and Actuators A: Physical 161 (2010) 158–163.

[7] Y.X. Liu, J.K. Liu, W.S. Chen, A cylindrical traveling wave ultrasonic motor using a circumferential composite transducer, IEEE Transactions on Ultrasonics, Ferroelectrics and Frequency Control 58 (2011) 2397–2404.

[8] Y. Liu, J. Liu, W. Chen, S. Shi, A u-shaped linear ultrasonic motor using longitudinal vibration transducers with double feet, IEEE Transactions on Ultrasonics, Ferroelectrics and Frequency Control 59 (2012) 981–989.